

Generalized stability analysis of shielded vortices

Luigi Bisanti^a, Pierre Brancher^a, Christophe Airiau^a

*a. Institut de Mécanique des Fluides de Toulouse (IMFT)
Allée du Pr Camille Soula, 31400 Toulouse, France*

Résumé :

Une analyse de stabilité généralisée d'une famille de tourbillons écrantés a été menée pour les faibles nombres de Reynolds. L'étude de stabilité temporelle modale permet de déterminer la courbe neutre. Ensuite, pour le cas particulier du tourbillon de Taylor, une étude en perturbation optimale dans le cas sous-critique révèle des amplifications transitoires à différents nombres d'onde azimutaux. Une étude au-dessus du seuil complète l'analyse aux temps courts. En dernier lieu, les effets de la diffusion de l'écoulement de base sont quantifiés pour un nombre de Reynolds de 100 : on montre que le mode le plus instable prédit par l'analyse de stabilité classique n'est pas nécessairement le plus dangereux aux temps courts.

Abstract :

A generalized stability analysis of a family of isolated vortices has been performed for low Reynolds numbers. The modal temporal stability analysis allows the neutral curve to be computed. Then, for the particular case of the Taylor vortex, a subcritical optimal perturbation analysis shows that transient energy growths can occur for various azimuthal wavenumbers. A study in the supercritical case completes the short-time analysis. Finally the effects of a diffusing base flow are investigated at Reynolds number 100: it is found that the most unstable mode predicted by the classical stability analysis is not necessarily the most dangerous at short times.

Keywords : Taylor vortex, flow instability, optimal perturbations

1 Introduction

The stability of columnar vortices have received a renewed attention in recent years, especially directing the efforts to reduce the aircraft trailing vortices hazard posed to following aircrafts. To complete the information given by the classical stability theory, several recent studies have focused on the transient dynamics since the modal stability theory is not able to predict the short-time evolution of perturbations. Indeed, if the asymptotically stable flow is governed by a non-normal operator, initial perturbations can experience transient amplifications [7] and eventually trigger a nonlinear, “bypass”, transition. Antkowiak and Brancher [1], Pradeep and Hussain [6] have shown and discussed the transient growth of perturbation in the asymptotically stable Lamb-Oseen vortex model, by applying the optimal perturbation approach initially developped in the context of wall-bounded shear flows. These authors have found that intense transient amplifications are possible for such vortex flows. The goal of the present work is to investigate whether transient amplifications can occur on the Taylor vortex model, belonging to the Carton-McWilliams family [3]. A preliminary modal stability analysis is necessary since such vortex is prone to centrifugal and inflectional instabilities [3]-[5]. The definition of neutral curve then allows to define and perform transient analyses in both subcritical and supercritical cases using the optimal perturbation approach via the direct-adjoint technique presented in Corbett and Bottaro [4] for the boundary layer case. In the last section, the effects of a diffusing base flow are investigated.

2 The base flow vortex model

First we study the asymptotic (*i.e.* long-time) stability properties of the Carton-McWilliams vortex model [3], a family of vortices in which an annulus of opposite vorticity is located at the periphery of the core and circulation vanishes over a distance depending on the steepness parameter α [3]. It is noteworthy that the presence of an off-axis peak in the axial vorticity profile and the vanishing circulation are related to azimuthal shear and centrifugal instability mechanisms respectively. Introducing cylindrical coordinates (r, θ, z) and referring to the characteristic length R_0 , the vortex radius, and the angular velocity Ω_0 on the vortex axis we define the Reynolds number as $Re = \Omega_0 R_0^2 / \nu$ and dimensionless vorticity and angular velocity are respectively

$$Z(r) = e^{-r^\alpha} (2 - \alpha r^\alpha) \quad \Omega(r) = e^{-r^\alpha}.$$

3 Temporal stability analysis

A classical modal stability analysis has been performed to examine the evolution of infinitesimal perturbations $\phi(r, \theta, z, t)$ of the steady incompressible base flow in the long-time asymptotic limit. The generic perturbation is expanded into normal form $\phi(r, \theta, z, t) = \hat{\phi}(r, t) e^{i(kz + m\theta)}$, where k and m are the axial and azimuthal wavenumbers, and introduced into the governing system, giving:

$$\mathbf{F}\mathbf{v} = \mathbf{L}\dot{\mathbf{v}} + \mathbf{C}\mathbf{v} - \frac{1}{Re}\mathbf{D}\mathbf{v} = \mathbf{0} \quad + \text{ b.c.} \quad (1)$$

This expression corresponds to the linearized Navier-Stokes equations combined with the continuity equation to rewrite the system in terms of the reduced variable $\mathbf{v} = (u_r, u_\theta)^T$. Then the classical eigenvalue problem formulation is obtained assuming an exponential time dependence for $\hat{\phi}(r, t) = \hat{\phi}(r) e^{-i\omega t}$, where ω denotes the complex angular frequency which is numerically computed. The

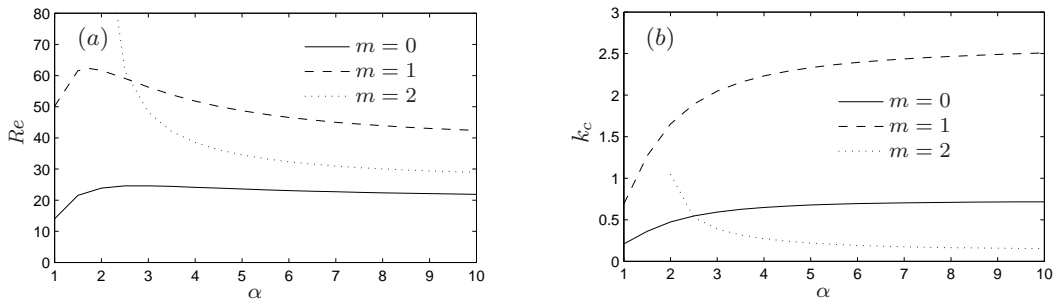


Figure 1: Stability of the Carton McWilliams vortex: (a) neutral curve and (b) critical axial wavenumber.

first step is to compute the points loci which delimit the stable-unstable regions, *i.e.* the neutral curve, as a function of the Reynolds number, the steepness parameter and the azimuthal wavenumber. Figure 1(a) plots the neutral curve for various azimuthal wavenumbers. Below these curves all the corresponding modes are stable. Figure 1(b) shows the critical axial wavenumber, defined as the wavenumber at which instability first appears. These results indicate that both critical Reynolds number and axial wavenumber asymptote a constant value at large α . Hereafter we focus on the Taylor vortex, characterized by a steepness parameter $\alpha = 2$. Figure 2 shows the stability curves for three azimuthal wavenumbers at various Reynolds numbers. We observe that more secondary instability branches appear as the Reynolds number increases. When k increases, the $m = 0$ and $m = 1$ modes become unstable and reach a maximum growth rate (the peak moving towards larger axial wavenumber as Reynolds number increases) before monotonically decreasing toward stability. This is in contrast with the inviscid flow behaviour, where the stability curves tend to reach a plateau value [8]. The effect of Reynolds number is not only to increase the growth rate but it also extends the instability band to a larger axial wavenumber range. On the other hand, the $m = 2$ modes are stable at Reynolds number 100, and unstable in the two-dimensional limit at larger Reynolds number. The

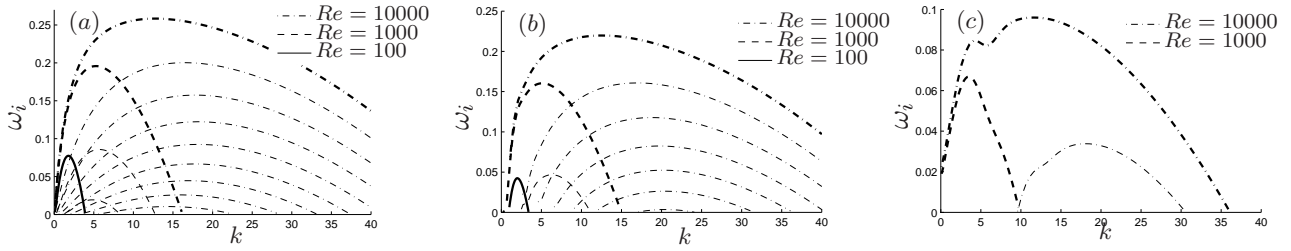


Figure 2: Growth rate as a function of k for various Reynolds numbers for (a) $m = 0$, (b) $m = 1$ and (c) $m = 2$. Bold curve corresponds to the primary (most) unstable mode.

stability curves presented here are in good agreement with the results of [5] and we confirm that the centrifugal instability is the dominant amplification mechanism in this long-time stability analysis.

Axisymmetric centrifugal modes are stationary whereas for $m > 1$ the rescaled angular frequencies ω_r/m are roughly constant (data not shown), as found in [8], and only weakly dependent on the Reynolds number.

4 Optimal perturbations

4.1 Analytical background

This section focuses on the transient dynamics of perturbations. We investigate potential mechanisms of transient growth through the computation of the initial perturbation that maximizes the energy gain $G(\tau) = E_\tau/E_0$, where

$$E_\tau = \frac{1}{2} \int_0^\infty (\bar{u}_r \cdot u_r + \bar{u}_\theta \cdot u_\theta + \bar{u}_z \cdot u_z) r dr$$

is the kinetic energy at a given time τ , the overbars denoting transpose conjugate quantities. In this context, the optimal perturbation is defined as the initial condition which maximizes the energy gain at a given time. Then the problem consists in maximizing an objective function, the energy gain, constrained by the linearized Navier-Stokes equations and the associated boundary conditions, where the initial condition \mathbf{v}_0 represents the control. In this work we use the scheme detailed in [4] to solve this problem. More precisely, it can be rewritten in an equivalent unconstrained form by introducing the following Lagrangian functional

$$\mathcal{L}(\mathbf{v}, \mathbf{v}_0, \mathbf{a}, \mathbf{c}) = G(\tau) - \langle \mathbf{F}(\mathbf{v}), \mathbf{a} \rangle - \langle \mathbf{H}(\mathbf{v}, \mathbf{v}_0), \mathbf{c} \rangle,$$

where we introduce the adjoint variables $\mathbf{a}(r, t)$ and $\mathbf{c}(r)$, playing the role of Lagrange multipliers, and where the last term of the functional assures that the initial state matches the control. The inner product appearing in (2) is defined as follows:

$$\langle \mathbf{p}, \mathbf{q} \rangle = \int_0^\tau \int_0^\infty (\bar{\mathbf{p}} \cdot \mathbf{q}) r dr dt + c.c.$$

Then the problem is to find the $(\mathbf{v}, \mathbf{v}_0, \mathbf{a}, \mathbf{c})$ set which corresponds to a stationary point for \mathcal{L} , thus providing a local extremum. If we set to zero the variation of the Lagrangian with respect to the state variable \mathbf{v} , the adjoint system (besides boundary conditions) is found for the costate \mathbf{a} :

$$\mathbf{F}^+ \mathbf{a} = -\mathbf{L} \dot{\mathbf{a}} + \mathbf{C}^+ \mathbf{a} - \frac{1}{Re} \mathbf{D} \mathbf{a} = \mathbf{0} \quad + b.c., \quad (2)$$

where \mathbf{C}^+ is the adjoint operator of \mathbf{C} , the resulting \mathbf{L} and \mathbf{D} operators being on the other hand self-adjoint. The problem is then solved via a direct-adjoint iterative algorithm (see [4] for more details), based on successive integrations of the direct (1) and adjoint (2) equations between $t = 0$ and $t = \tau$.

4.2 Subcritical optimal perturbations

For the present base flow, it is possible to show that the advection operator \mathbf{C} is not self-adjoint, which suggests that transient growth for perturbations is possible [7]. We first investigate this possibility by focusing on the subcritical case as defined in figure 1. We observe that no transient amplification occurs for the axisymmetric modes (data not shown). It is important to outline that in this case the system is nevertheless non-normal (unlike the particular case $m = 0$ and $k = 0$) and transient amplifications are still possible, as showed in [2] and [6] for the Lamb-Oseen vortex at larger Reynolds numbers. They are not observed here because of the present low Reynolds number limit ($Re < 25$) given by neutral curve. In other words, considering the perturbations energy integral balance, the production term is not able to counter the dissipative one, which plays the dominant role.

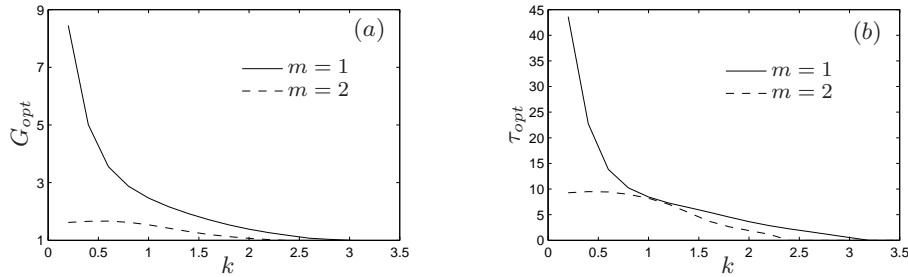


Figure 3: Optimal gain (a) and associated optimal time (b) as functions of the axial wavenumber k for $m = 1$ and $m = 2$ at $Re = 50$.

Figure 3 shows that subcritical transient amplification involves the $m = 1$ and $m = 2$ modes, although the energy gain does not reach very high levels, once again because the neutral curves in figure 1 limit our analysis to relatively low Reynolds numbers. In particular, the optimal gains and the associated optimal times are plotted as functions of the axial wavenumber, the optimal gain corresponding to the maximum gain $G_{opt} = \max_{\tau} G(\tau)$ which occurs at the optimal time τ_{opt} . For $m = 1$ we observe that amplifications become more important, and occur at later times, as the axial wavelength increases. No amplification is observed at small wavelengths, more precisely for $k > 3$. By comparison, the $m = 2$ case shows less important growths than for $m = 1$ and presents a maximum in the energy gain for $k \approx 0.6$. The optimal time differ significantly from the $m = 1$ case at small wavelengths, but the kinetics is faster at large axial wavelengths.

4.3 Supercritical optimal perturbations

This section focuses on the perturbation of the Taylor vortex in the unstable regime. It is known that if the initial condition is defined as the most unstable eigenmode, the time evolution of the perturbation energy will exactly correspond to the exponential growth of this eigenmode. On the other hand, if we impose any initial perturbation, we expect the most unstable mode to emerge only after a transient, at sufficiently large times. Moreover the perturbation energy at a given long-time $\bar{\tau}$ will not necessarily be the same as reached at $\bar{\tau}$ in the case where the most unstable eigenmode is directly injected initially.

In order to quantify this behavior, we introduce $g(\tau) = \log(G_{op}(\tau)) - \log(G_{ip}(\tau))$ as a measure of the gain, where $G_{op}(\tau)$ is the gain at the final time τ when the flow is optimally perturbed and $G_{ip}(\tau) = e^{2\omega_i\tau}$ is the gain at time τ when the flow is perturbed through the most unstable eigenmode predicted by the preliminary stability analysis. With this definition, we expect that the gain $g(\tau)$ asymptotes a constant value for sufficiently large τ . Yet it can reach larger values at short times, then showing a peak (the optimal gain g_{opt}) for a given τ (the optimal time). Figure 4 (where we adopt the notation $g_i = g|_{m=i}$ and similarly for the optimal time) answers positively this question, showing for $m = 0$ some maximum gains at short time. In particular figure 4(a) plots the gain as a function of τ for $k = 4.1$ (which corresponds to the maximum growth rate at Reynolds number 500), where the peak at $\tau = 5$ is well defined. We can observe that the optimal gain and the optimal time are both monotonously decreasing functions of the axial wavenumber and they converge to a

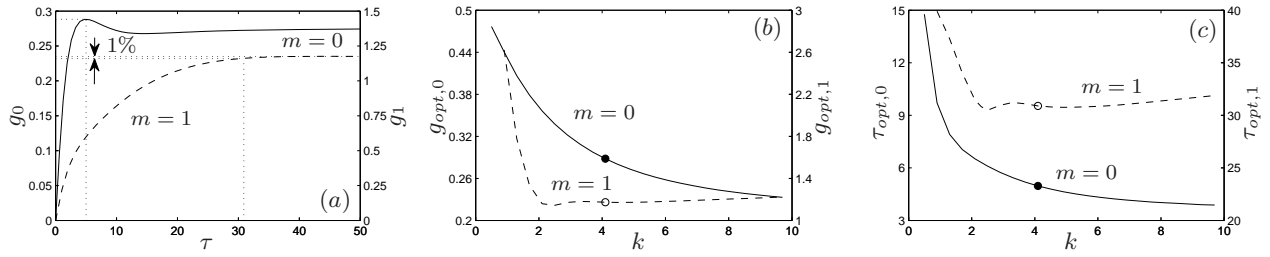


Figure 4: (a) Supercritical gain $g_i = g|_{m=i}$ as function of τ at Reynolds number 500 and $k = 4.1$; (b)-(c) optimal supercritical gain and respective optimal time as function of k at $Re = 500$. The filled and hollow circles correspond to optimal gain (and optimal time) emphasized in (a) for $m = 0$ and $m = 1$ respectively.

finite value as k increases. On the other hand, for $m = 1$, such local maximum is not observed and we define the optimal time as the time at which the energy growth reaches 99% of the asymptotic energy gain ($G(t \rightarrow \infty)$, cf. figure 4(a)), that is therefore the optimal gain. Figure 4(c) shows that the amplification mechanisms kinetics for $m = 0$ is faster than for $m = 1$.

5 Effect of the base flow diffusion

The classical linear stability theory requires the base flow to be steady and the results are reliably extrapolated to the case of a diffusing base flow if the characteristic time of the perturbation evolution is much smaller than the diffusive time $\tau_D \approx \mathcal{O}(Re)$. For a diffusing base flow, in the limit $t \rightarrow \infty$, we expect that the energy associated with the perturbation eventually tends to zero, since the production and the spatial energy redistributing terms on the energy integral balance vanish, so that the dynamics is exclusively controlled by the dissipative term.

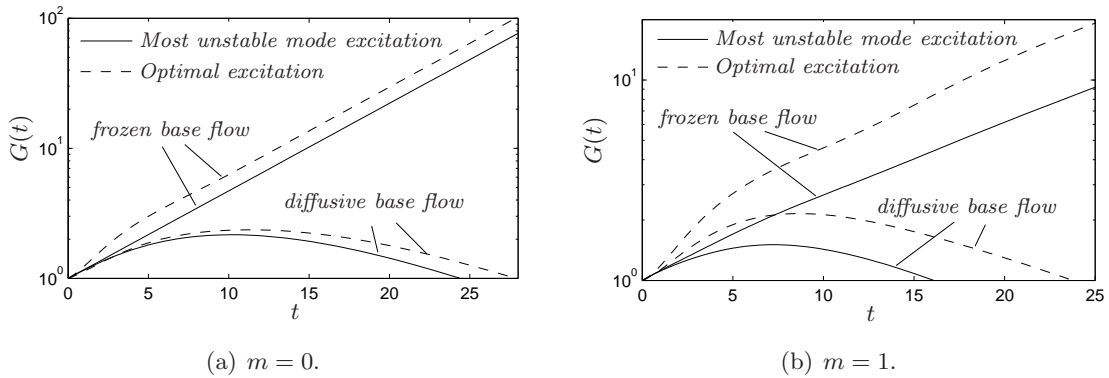


Figure 5: Comparison of the temporary evolution of the gain for a final time $\tau_{fin} = 30$ for a frozen base flow and a diffusive one at $Re = 100$, $k = 1.8$, $m = 0$ (a) and $m = 1$ (b).

On the other hand, the method used to compute the optimal perturbation does not require to freeze the base flow, so we can analyse the time evolution of a perturbation injected on a diffusing Taylor vortex, characterized by the non-dimensional angular velocity $\Omega(r, t) = [\exp(-r^2/(1 + 4t/Re))]/(1 + 4t/Re)$. Figure 5 shows the time evolution of the gain at Reynolds number 100, for axial wavenumber $k = 1.8$ (which corresponds to the maximum growth rate at $Re = 100$ and $m = 0$, cf. figure 2(a)) when the initial condition is the most unstable eigenmode (solid curves) or the optimal perturbation (dotted curves), where in the latter case we set the terminal time $\tau = 30$. The diffusing base flow data show a trend in contrast with what has been observed previously: the mechanisms activated here by viscosity can play an important role even on a time scale of one order less than τ_D .

Figure 6(a) plots the optimal gain as function of the axial wavenumber k at Reynolds number 100. While the long-time analysis predicts that $m = 0$ is the most unstable, the short-time analysis confirms

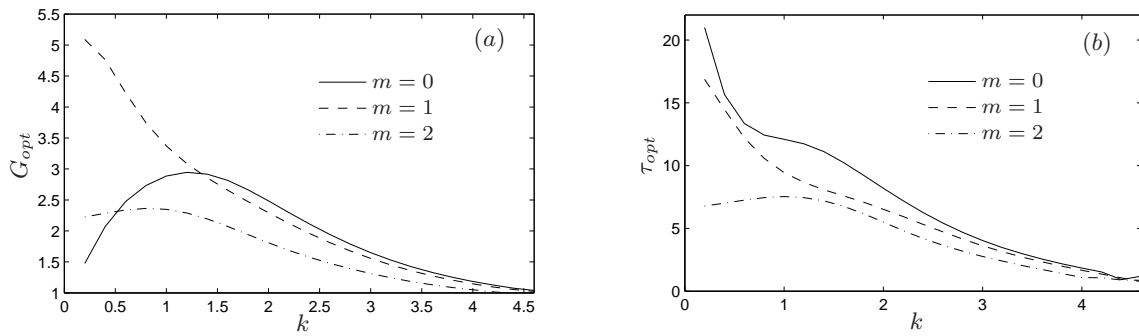


Figure 6: Optimal gain (a) and associated optimal time (b) as functions of the axial wavenumber k at various azimuthal wavenumbers m for the diffusive base flow at $Re = 100$.

it for $k > k' = 1.3$ but shows that, for larger axial wavelengths, the mode $m = 1$ is in fact the most dangerous ($[G_{m=1}/G_{m=0}]_{k=0.2} \approx 3.4$). There is even a second cut-off wavenumber ($k'' = 0.5$) below which the most unstable mode found by the stability analysis becomes the less dangerous one in the transient analysis. It is noteworthy that for $k < 1$ there is a range of axial wavenumbers where the $m = 1$ modes, that the temporal stability analysis predicts as stable, experience a greater transient growth than the unstable $m = 0$ modes.

6 Conclusions and perspectives

We have analyzed the transient dynamics of perturbation of the Taylor vortex by an optimal perturbation approach, concluding that transient energy growth occurs in both subcritical and overcritical configurations. We observed that, for a diffusing base flow, there is an axial cutoff wavenumber below which the most dangerous mode given by the short-time analysis is not the axisymmetric $m = 0$ as predicted by long-time stability analysis, but rather bending modes at $m = 1$. The physical analysis of the spatial structure and time evolution of the optimal perturbations is currently under way. Moreover, an analytical model which completes the stability results accounting on the base flow diffusion is currently developed.

References

- [1] Antkowiak, A., Brancher, P. 2004 Transient energy growth for the Lamb-Oseen vortex. *Phys. Fluids* **16** (1), L1–L4
- [2] Antkowiak, A., Brancher, P. 2007 On vortex rings around vortices: an optimal mechanism. *J. Fluid Mech.* **578**, 295–304
- [3] Carton, X., McWilliams, J. 1989 Barotropic and baroclinic instabilities of axisymmetric vortices in a quasi-geostrophic model. in *Mesoscale/Synoptic Coherent Structures in Geophysical Turbulence* edited by J. Nihoul and B. Jamart (Elsevier, New York), 225–244.
- [4] Corbett, P., Bottaro, A. 2001 Optimal linear growth in swept boundary layers. *J. Fluid Mech.* **435**, 1–23
- [5] Gallaire, F., Chomaz, J. M. 2003 Three-dimensional instability of isolated vortices. *Phys. Fluids* **15** (8) 2113–2126
- [6] Pradeep, D. S., Hussain, F. 2006 Transient growth of perturbations in a vortex column. *J. Fluid Mech.* **550**, 251–288
- [7] Schmid, P. J., Henningson, D. S. 2001 *Stability and Transition in Shear Flows*. Springer.
- [8] Smyth, W. D., McWilliams, J. C. 1998 Instability of an Axisymmetric Vortex in a Stably, Rotating Environment. *Theor. Comp. Fluid Dyn.* **11**, 305–322